



HAL
open science

Deubiquitylase UCHL3 regulates bi-orientation and segregation of chromosomes during mitosis

Katerina Jerabkova, Yongrong Liao, Charlotte Kleiss, Sadek Fournane, Matej Durik, Arantxa Agote-arán, Laurent Brino, Radislav Sedlacek, Izabela Sumara

► **To cite this version:**

Katerina Jerabkova, Yongrong Liao, Charlotte Kleiss, Sadek Fournane, Matej Durik, et al.. Deubiquitylase UCHL3 regulates bi-orientation and segregation of chromosomes during mitosis. *FASEB Journal*, 2020, 34 (9), pp.12751 - 12767. 10.1096/fj.202000769r . hal-03097592

HAL Id: hal-03097592

<https://hal.science/hal-03097592>

Submitted on 5 Jan 2021

HAL is a multi-disciplinary open access archive for the deposit and dissemination of scientific research documents, whether they are published or not. The documents may come from teaching and research institutions in France or abroad, or from public or private research centers.

L'archive ouverte pluridisciplinaire **HAL**, est destinée au dépôt et à la diffusion de documents scientifiques de niveau recherche, publiés ou non, émanant des établissements d'enseignement et de recherche français ou étrangers, des laboratoires publics ou privés.

RESEARCH ARTICLE

Deubiquitylase UCHL3 regulates bi-orientation and segregation of chromosomes during mitosis

Katerina Jerabkova^{1,2,3,4,5,6} | Yongrong Liao^{1,2,3,4} | Charlotte Kleiss^{1,2,3,4} |
 Sadek Fournane^{1,2,3,4} | Matej Durik^{1,2,3,4} | Arantxa Agote-Arán^{1,2,3,4} |
 Laurent Brino^{1,2,3,4} | Radislav Sedlacek^{5,6,7} | Izabela Sumara^{1,2,3,4}

¹Institut de Génétique et de Biologie Moléculaire et Cellulaire (IGBMC), Department of development and stem cells, Illkirch, France

²Centre National de la Recherche Scientifique UMR 7104, Strasbourg, France

³Institut National de la Santé et de la Recherche Médicale U964, Strasbourg, France

⁴Université de Strasbourg, Strasbourg, France

⁵Laboratory of Transgenic Models of Diseases, Institute of Molecular Genetics of the CAS, v.v.i., Vestec, Czech Republic

⁶Faculty of Science, Charles University, Prague, Czech Republic

⁷Czech Centre for Phenogenomics, Institute of Molecular Genetics of the CAS, v.v.i., Vestec, Czech Republic

Correspondence

Radislav Sedlacek, Laboratory of Transgenic Models of Diseases, Institute of Molecular Genetics of the CAS, v.v.i., Vestec, Czech Republic.
 Email: radislav.sedlacek@img.cas.cz

Izabela Sumara, Institut de Génétique et de Biologie Moléculaire et Cellulaire (IGBMC), Illkirch, France.
 Email: sumara@igbmc.fr

Present address

Laurent Brino, Ksilink, Strasbourg, France

Funding information

Agence Nationale de la Recherche (ANR), Grant/Award Number: ANR-10-LABX-0030-INRT; Ligue Contre le Cancer; China Scholarship Council (CSC); Czech Academy of Sciences, Grant/Award Number: RVO68378050; Ministry of Education, Youth, and Sports of the Czech Republic, Grant/Award Number:

Abstract

Equal segregation of chromosomes during mitosis ensures euploidy of daughter cells. Defects in this process may result in an imbalance in the chromosomal composition and cellular transformation. Proteolytic and non-proteolytic ubiquitylation pathways ensure directionality and fidelity of mitotic progression but specific mitotic functions of deubiquitylating enzymes (DUBs) remain less studied. Here we describe the role of the DUB ubiquitin carboxyl-terminal hydrolase isozyme L3 (UCHL3) in the regulation of chromosome bi-orientation and segregation during mitosis. Downregulation or inhibition of UCHL3 leads to chromosome alignment defects during metaphase. Frequent segregation errors during anaphase are also observed upon inactivation of UCHL3. Mechanistically, UCHL3 interacts with and deubiquitylates Aurora B, the catalytic subunit of chromosome passenger complex (CPC), known to be critically involved in the regulation of chromosome alignment and segregation. UCHL3 does not regulate protein levels of Aurora B or the binding of Aurora B to other CPC subunits. Instead, UCHL3 promotes localization of Aurora B to kinetochores, suggesting its role in the error correction mechanism monitoring bi-orientation of chromosomes

Abbreviations: APC/C, anaphase-promoting complex/cyclosome; BAP1, BRCA1-associated protein 1; BubR1, Bub1-related 1 kinase; CPC, chromosomal passenger complex; DAPI, 4',6-diamidino-2-phenylindole dihydrochloride; DUBs, deubiquitylases; MAD2, mitotic arrest deficient 2; MCAK, mitotic centromere-associated kinesin; MCC, mitotic checkpoint complex; MT-KT, microtubule-kinetochore; PP1 γ , protein phosphatase 1 gamma; SAC, spindle assembly checkpoint; STLC, S-trityl-L-cysteine; TCID, 4,5,6,7-tetrachloro-1*H*-indene-1,3(2*H*)-dione; UCH, C-terminal hydrolases; UCHL3, ubiquitin carboxyl-terminal hydrolase isozyme L3.

Katerina Jerabkova and Yongrong Liao contributed equally to this work

This is an open access article under the terms of the Creative Commons Attribution-NonCommercial-NoDerivs License, which permits use and distribution in any medium, provided the original work is properly cited, the use is non-commercial and no modifications or adaptations are made.

© 2020 The Authors. The FASEB Journal published by Wiley Periodicals LLC on behalf of Federation of American Societies for Experimental Biology

LM2015040; IGBMC; CNRS; Fondation ARC pour la recherche sur le cancer; Institut National du Cancer (INCa); USIAS; Programme Fédérateur Aviesan; INSERM; Sanofi iAward Europe

during metaphase. Thus, UCHL3 contributes to the regulation of faithful genome segregation and maintenance of euploidy in human cells.

KEYWORDS

Aurora B, DUBs, chromosome alignment, chromosome segregation, mitosis

1 | INTRODUCTION

Faithful chromosome segregation during mitosis ensures genome stability and defects in this process may lead to an imbalance in chromosomal composition named aneuploidy or polyploidy, which have been causally linked to cellular transformation.¹ The kinetochore is a large proteinaceous structure built onto centromere regions of sister chromatids of all chromosomes where spindle microtubules attach, thereby driving faithful sister chromatid separation at the transition from metaphase to anaphase. At the kinetochore, the surveillance mechanism called the spindle assembly checkpoint (SAC) (also known as the mitotic checkpoint) monitors correct microtubule-kinetochore (MT-KT) attachments and bi-orientation of chromosomes.² The SAC inhibits the onset of chromosome segregation during anaphase until all chromosomes form proper attachments with the mitotic spindle (bi-orientation or amphitelic attachments), where each kinetochore is bound to microtubules emanating from the opposite spindle poles.^{3,4} Unattached kinetochores create a binding platform for various SAC proteins including mitotic arrest deficient 2 (MAD2), budding uninhibited by benzimidazoles 3 (Bub3), and Bub1-related 1 kinase (BubR1) proteins, which form the mitotic checkpoint complex (MCC) able to sequester the Cdc20 protein. Cdc20 represents the co-activator and the substrate-specific adaptor of the E3-ubiquitin ligase anaphase-promoting complex/cyclosome (APC/C), which ubiquitylates and targets securin and cyclin B proteins for 26S proteasomal degradation, thereby triggering anaphase onset.⁵ The kinetochore attachment defects such as syntelic (attached to the single pole) or monotelic (mono-oriented) attachments, prevent SAC satisfaction and inhibit chromosome segregation, often leading to prolonged mitotic arrest and ultimately to cell death. Importantly, such defects in microtubule attachments to kinetochores can be repaired by the error correction mechanism, which allows for selective destabilization of these erroneous configurations and for stabilization of bi-oriented attachments.⁶ One of the main factors driving error correction is the mitotic kinase Aurora B.^{7,8} Aurora B is a catalytic subunit of the so-called chromosomal passenger complex (CPC), which dynamically localizes to centromeres, kinetochores, and microtubules during mitotic progression.⁹ Downregulation or inhibition of Aurora B stabilizes incorrect attachments^{7,8,10-12} and many microtubule-associated Aurora B substrates were identified.¹³ For instance, the activity of Aurora B is required for the kinetochore localization and

function of mitotic centromere-associated kinesin (MCAK) (also known as Kif2C), which acts as a microtubule depolymerase on incorrectly formed MT-KT attachments.¹⁴⁻²⁰ The recruitment of the kinesin CENP-E to kinetochores is regulated by Aurora B, playing an important role in the conversion from initial lateral MT-KT attachments to the end-on attachments and thereby in the bi-orientation of the chromosomes.^{11,21} Conversion of the lateral to the end-on attachments as well as stabilization of the bi-oriented attachments is also controlled by the astrin-SKAP complex, which is antagonized by the action of Aurora B.^{22,23} It has been initially suggested that the role of Aurora B in the regulation of SAC is indirect, namely that in the absence of spindle-exerted tension across the centromeres, the error correction mechanism is activated leading to destabilization of erroneous MT-KT attachments and in turn to SAC potentiation.^{24,25} However, accumulating evidence suggests the important direct role of Aurora B in SAC signaling²⁶ also through kinetochore recruitment of numerous SAC proteins.^{10,11,27-29} Thus, Aurora B is an upstream factor playing critical roles in SAC signaling and error correction during mitosis.

Aurora B is targeted for 26S proteasomal degradation by APC/C-mediated ubiquitylation during late mitosis³⁰ but its mitotic functions are also controlled by non-degradative ubiquitylation.³¹⁻³⁵ Indeed, many proteolytic and non-proteolytic ubiquitylation pathways were identified to play important roles during mitotic progression by determining the fates of ubiquitylated substrate proteins.³⁶⁻³⁸ While mitotic E3-ubiquitin ligases are widely investigated, our knowledge of mitosis-specific roles of DUBs remains rather limited. Here, using unbiased screening approaches, we identify an unexpected role of the deubiquitylase UCHL3 which exerts specific function on chromosome bi-orientation and segregation during mitosis of human cells.

2 | MATERIALS AND METHODS

2.1 | Reagents and antibodies

TCID (4,5,6,7-tetrachlorodindan-1,3-dione) UCHL3 inhibitor (Tebu-Bio, Ref. 27720-1) was used at 2 μ M working concentration. Monastrol (Sigma-Aldrich, Ref. M8515) and 4',6-Diamidino-2-phenylindole dihydrochloride (DAPI) (Sigma-Aldrich, Ref. D8417). S-Trityl-L-cysteine (STLC), (Enzo Life Sciences, Ref. ALX-105-011-M500), proteasomal

inhibitor MG132 (Tocris bioscience, No. 1748), protease inhibitors (Roche, cOmplete EDTA-free Protease Inhibitor Cocktail).

UCHL3 antibody was produced in collaboration with the IGBMC antibody facility using immunized rabbits and purified with SulfoLink resins according to the manufacturer's protocol. The astrin polyclonal rabbit antibody was a kind gift from Ulrike Gruneberg (Cancer Research, UK). Commercial antibodies: mouse monoclonal BubR1 (BD Biosciences, 612502 clone 9/BubR1), mouse monoclonal α -tubulin (Sigma Aldrich, T5168), human polyclonal CREST (Antibodies Incorporated, 15 234), rabbit polyclonal Aurora B (Abcam ab2254), mouse monoclonal UCHL3 (Sigma Aldrich, clone H7171), mouse monoclonal CENP-E (Thermo Scientific, MA1-5758), rabbit polyclonal GFP (Abcam, ab290), cyclin B1 (GNS1) (Santa-Cruz, sc-245), β -actin (Sigma Aldrich, A2228), PP1 γ (Santa Cruz, sc-517354), HOIP (Abcam, ab125189). MAD2L1 (GeneTex, GTX104680, survivin (Abcam, ab469).

2.2 | Plasmids

All GFP plasmids used were cloned into pEGFP-N1 plasmid (Clontech): pEGFP-N1, pEGFP-N1-UCHL3-WT, pEGFP-N1-UCHL3-C/S. UCHL3 (NCBI, variant2 NM_006002.4) was cloned from human cDNA lacking the 3'UTR region. UCHL3 catalytic dead mutant has cysteine 95 residue mutated to serine by G > C base exchange in the cysteine codon. For Immunoprecipitation experiments, N-terminally tagged pEGFP-Aurora B³¹ vector was used.

2.3 | Cell culture and synchronization of cells

All cell lines were purchased from ATCC and cultured at 37°C in a 5% CO₂ humidified incubator, if not stated otherwise. HeLa Kyoto (human cervix carcinoma) cells were cultured in high glucose DMEM-GlutaMAX containing 4.5 g/L glucose, 10% fetal calf serum, 1% penicillin, and streptomycin. Human primary lung fibroblasts (IMR90) were cultured in EMEM containing non-essential AA, 2 mM L-glutamine, 1 mM sodium pyruvate, 1500 mg/L sodium bicarbonate, 10% fetal calf serum, and gentamycin. Dld1 cells were cultured in RPMI-1640 medium containing 2 mM L-glutamine, 10 mM HEPES, 1 mM sodium pyruvate, 4.5 g/L glucose, 1.5 g/L sodium bicarbonate, 10% fetal calf serum and gentamycin. Cells were trypsinized, counted in Neubauer chamber, and seeded on 9-15 mm glass coverslips (Menzel-Glaser) in 24-well plates at a density of 15 000 cells per well for all immunofluorescence experiments. To synchronize cells in prometaphase STLC (50 mM/DMSO) was diluted

in medium to 5 μ M and cells were treated for 16 hours. Monastrol (100 mM/DMSO) was diluted to 100 μ M and used for 16 hours. Monastrol washout: upon incubation, cells were washed 5 \times with warm medium and released in fresh culture medium for different time periods as indicated in respective figures. Monastrol release: upon incubation, cells were washed 5 \times with warm medium and released for 90 minutes to MG132 (50 μ M) containing medium to arrest the cells in metaphase. Thymidine (200 mM/H₂O) was used at 2 mM, cells were treated 16 hours, washed three times, released for 8 hours, and treated again for 16 hours with thymidine followed by three washes. Mitotic cells were observed 8.5 hours after the second release.

2.4 | Stable cell lines

HeLa Kyoto stable cell line expressing GFP tag fused to the endogenous Aurora B locus (HK-ZFN-AURKB-mEGFP referred to as Aurora B-GFP) and the HeLa Kyoto H2B-mCherry tubulin-GFP cell line were purchased from Cell Line Service (CLS), Germany. Dld1-mCherry cell line³⁹ was a kind gift from Don Cleveland and HeLa Kyoto GFP-CENP-A cell line was a kind gift from Jason Swedlow.

UCHL3 stable cell lines were generated in HeLa Kyoto cells by random integration of GFP-UCHL3 plasmids. Three lines were generated: GFP-HeLa expressing empty pEGFP-N1 plasmid as a control, GFP-WT-UCHL3 expressing wild-type sequence of UCHL3, and GFP-C/S-UCHL3 expressing catalytic dead mutant of UCHL3. Expression levels of different proteins were estimated by western blot. Cell lines expressing near endogenous levels of UCHL3 proteins were chosen for immunoprecipitation experiments.

For retroviral-mediated silencing of genes induced by stable expression of short hairpin RNA (shRNA) targeting UCHL3 ATAGAAGTTTGCAAGAAGTTTA and a control sequence TAATCAGAGACTTCAGGCGG (targeting Firefly luciferase) was cloned into an LMP backbone. This plasmid contains long terminal repeats and retroviral packaging signal necessary for the virus production and PKG promoter-driven expression of a cassette coding for puromycin resistance and GFP. Furthermore, for improved production of the shRNA, it contains a cassette with U6 promoter-driven expression of miR30 microRNA context into which the designed shRNA sequences are cloned. Retrovirus was produced by transiently transfecting the Phoenix packaging cell line (G. Nolan, Stanford University, Stanford, CA) with the prepared plasmids. Supernatant was collected, filtered to remove cellular debris, polybrene was added and the supernatant was used to infect HeLa cells or Dld1 cells overnight. After 2 days, cells were selected using puromycin (1 mg/mL) for 48 hours. After selection, the presence of replicatively competent retrovirus was excluded using qPCR. The knockdown of UCHL3 was validated using western blotting.

2.5 | Generation of UCHL3^{-/-} cell lines by CRISPR/Cas9 genome editing system

For generating HeLa UCHL3^{-/-} cell lines, guide RNA (gRNA) was designed by online software Benchling (<https://www.benchling.com/>), 5'-CAAACAATCAGCAATGCCTG-3' and 5'-TGAAGTATTCAGAACAGAAG-3' and cloned into pX330-P2A-EGFP (Addgene) through ligation using T4 ligase (New England Biolabs). HeLa-Kyoto cells were transfected using Lipofectamine™ 2000 Transfection Reagent (Thermo Fisher Scientific), 24 hours after transfection, GFP-positive cells were collected by FACS (BD FACS Aria II) and seeded into 96-well plates. Obtained UCHL3^{-/-} single-cell clones were examined by western blotting and sequencing of PCR-amplified targeted fragment by Phusion polymerase (Thermo Scientific). The PCR amplification primers were: 5'-CTGTAACGTGATCGTACAAA-3' (forward) and 5'-GAATTAGAGCACCACTACT-3' (reverse).

2.6 | siRNA experiments

Cells were transfected by Oligofectamine at the final concentration 30 nM of the siRNA: Non-targeting individual siRNA-2 5'-UAAGGCUAUGAAGAGAUAC-3' (Dharmacon), UCHL3 siRNA-1 5'-CAGCAUAGCUUGUCAUAA-3', UCHL3 siRNA-2 5'-GCAAUUCGUUGA UGUUAU-3', UCHL3 3'UTR siRNA 5'-CUGCCAUAACACUAACUCAA-3', Ku80 siRNA (XRCC5 Dharmacon On-Target Plus) based on the manufacturer's instructions. For rescue experiments, cDNAs and siRNAs were co-transfected by Lipofectamine 2000 according to manufacturer's instructions.

2.7 | Immunoprecipitations

HeLa cells stably expressing GFP-UCHL3 proteins were cultured, synchronized with STLK and harvested in 1 mL of lysis buffer (10 mM Tris HCl pH 7.5, 150 mM NaCl, 0.5 mM EDTA, 0.5% NP-40, protease inhibitor cocktail) per four 10 cm dishes in each condition. GFP-trap agarose beads (Chromotek) were blocked overnight in 3% BSA diluted in wash buffer (10 mM Tris HCl pH 7.5, 150 mM NaCl, 0.5 mM EDTA, protease inhibitor cocktail), washed three times in lysis buffer and incubated with 10 mg of cell extracts overnight, rotating at 4°C. Before elution, the beads were washed five times for 5 minutes with 1 mL of washing buffer (centrifugation 500 g, 2 minutes). The proteins were eluted from beads by boiling in 2× Laemmli SDS sample buffer (Bio-Rad) for 15 minutes. Samples were analyzed by western blotting.

For immunoprecipitation under denaturing conditions, UCHL3^{+/+} and UCHL3^{-/-} HeLa cells were transfected

with GFP-Aurora B or pEGFP-N1 and synchronized by monastrol for 18 hours. Cells were lysed with Urea lysis buffer (8M Urea, 300 mM NaCl, 50 mM Na₂HPO₄, 50 mM Tris-HCl, 1 mM PMSF, pH 8) and sonicated, supernatants were cleared by centrifugation at 16 000 g for 15 minutes and incubated with GFP-Trap agarose beads (Chromotek) overnight at 4°C. Beads were washed by Urea lysis buffer, eluted in 2× Laemmli buffer and analyzed by western blotting.

2.8 | Western blot analysis

To isolate proteins, cells were scraped, pelleted by centrifugation at 4°C and washed twice in PBS. Lysates were prepared using RIPA buffer (50 mM Tris-HCl pH7.5, 150 mM NaCl, 1% Triton X-100, 1 mM EDTA) supplemented with 1 mM NaF, 1 mM DTT and protease inhibitor cocktail Complete. Cells were lysed on ice by mechanical disruption with a needle (26G) and centrifuged at 10 000 g for 30 minutes at 4°C. Protein concentration of supernatant was measured by Bradford assay (Bio-Rad). Samples were boiled for 10 minutes in Laemmli buffer with β-Mercaptoethanol (Bio-Rad), resolved on 10% polyacrylamide gels or pre-cast gradient gels (Thermo Scientific, NW04120BOX) and transferred onto PVDF membrane (Millipore) using semi-dry transfer unit (Amersham). About 5% of non-fat milk was used for blocking and for antibody dilutions. TBS-T (25 mM Tris-HCl, pH 7.5, 150 mM NaCl, 0.05% Tween) was used for washing.

2.9 | Quantitative PCR analysis

RNA was isolated from HeLa cells using a kit from Macehery Nagel and reversed transcribed by qScript cDNA SuperMix (Quanta Bio) according to the protocols. For the qPCR 20 ng of cDNA were used per reaction and amplified with SYBR Green I master mix from Roche (04 887 352 001) at 60°C and values were normalized to GAPDH. Human Ku80 primers: Fwd GCTAATCCTCAAGTCGGCGT, Rev CAGCATTCAACTGTGCCTCG, GAPDH primers: Fwd CACCCAGAAGACTGTGGATGG, Rev GTCTACATGGCAACTGTGAGG.

2.10 | Immunofluorescence microscopy

Cells were washed once in PBS and fixed in 4% PFA for 17 minutes at room temperature (RT), washed three times in PBS and permeabilized in 0.5% NP-40 for 5 minutes, followed by three washes in PBS-T and blocking in 3% BSA in PBS-T for 90 minutes at RT or at 4°C overnight. Primary antibodies were diluted in the blocking buffer and incubated

for 2 hours at RT, washed three times for 5 minutes in PBS-T and incubated with secondary antibodies at 1:5000 dilution for 1 hour at RT in the dark. Cells were washed three times for 10 minutes in PBS-T and incubated with DAPI diluted in PBS at final concentration 1 $\mu\text{g}/\text{mL}$ for 10 minutes at RT, followed by two washes in PBS-T. Cover slips were mounted on glass slides using Mowiol and dried overnight. High-resolution images were taken using Leica CSU-W1 spinning disc confocal microscope with Live SR module at 100 \times magnification and were processed in Image J followed by the analysis using CellProfiler as described below.

For analysis of the kinetochore proteins, prior to fixation, cells were incubated in extraction buffer (PHEM, 1 mM PMSF, 1 mM ATP, 0.5% Triton X-100) for 3 minutes at 37°C and fixed after in 4% PFA for 2 minutes at 37°C followed by two times for 5 minutes incubation with 0.5% Triton in PBS at 37°C. Cells were blocked in 3% BSA in PBS-T, followed the standard IF protocol from this step onwards. PHEM buffer (pH 6.9, PIPES 45 mM, HEPES 45 mM, EGTA 10 mM, MgCl₂ 5 mM).

For the quantification of the misaligned chromosomes in fixed samples, cells were stained with DAPI. The experiments were performed in a blinded setup. For each category, the number of cells with aligned and misaligned chromosomes was counted and the percentage of total cells was quantified. In each experiment between 200 and 800 cells per condition were counted.

2.11 | Live video imaging

Cells were seeded in a glass-bottom dish, 30 mm diameter with four compartments, and synchronized with monastrol or thymidine. For acquisition, Leica CSU-W1 spinning disk, 63 \times objective, water immersion were used with time frames of 5 minutes and Z step 2 μm . Cells were placed into a humid heated chamber with 5% CO₂ and 80% humidity in the microscope and for monastrol release, cells were rinsed five times with warm medium to wash out the monastrol. Eight positions were selected for each condition and pictures were taken for 4 hours. Images were processed in ImageJ and maximum Z-projections were created.

2.12 | CellProfiler data analysis

Cell Profiler 3.1.8 was used to analyze the immunofluorescent images. Irregular nuclei: The form factor was calculated as $4*\pi*Area/Perimeter^2$. Primary objects (nuclei) were identified based on the DAPI channel and the form factor for each nucleus was calculated in all conditions. Threshold was set to discriminate between regular and irregular nuclei and the percentage of irregular nuclei was plotted. Relative kinetochore

intensity was quantified based on the immunofluorescence image of CREST staining (kinetochore regions). The mean intensity of CREST and protein of interest (POI): BubR1, Astrin was measured in the selected area and the ratio of the POI intensity to the CREST intensity (POI/ CREST) was calculated and the values were normalized to the control condition (control = 1). Spatial attributes were assigned manually to the individual chromosomes (C- centered, P- polar). Aurora B, MCAK, and CREST objects were selected based on an intensity threshold. The number of objects and their area were measured together with the mean and integrated intensities for Aurora B and MCAK. Two focus planes were chosen for analysis from each Z-stack.

2.13 | Statistics

To statistically evaluate the data, the parametric One-Sample *T*-test was used for samples normalized to the control and parametric Two-sample *T*-test was used for the rest of the conditions. Values were considered significantly different if $P < .05$ and stars were assigned as follows: $P < .05$ *, $P < .01$ **, $P < .001$ ***, $P < .0001$ ****. In all graphs, results are shown as mean \pm SEM (or SD) of at least three independent experiments. Details for each graph are listed in figure legends.

3 | RESULTS

3.1 | UCHL3 controls euploidy of human cells

Many E3-ubiquitin ligases and ubiquitin-binding proteins are known to regulate mitotic progression but specific mitotic functions of deubiquitylating enzymes (DUBs) remain less studied. To identify DUBs that control cell division and euploidy of human cells, we performed a high content visual siRNA screen in HeLa cells for approximately 100 known and predicted human DUBs using the established approach previously described in our laboratory for the ubiquitin-binding proteins.³⁵ We scored for terminal phenotypes of multilobed nuclei and multinucleation often resulting from defects in chromosome segregation and cytokinesis such as those observed upon downregulation of Aurora B and UBASH3B³⁵ (Figure 1A). Downregulation of the top DUB hit (Table S1), ubiquitin carboxyl-terminal hydrolase isozyme L3 (UCHL3) showed similar strong nuclear atypia relative to the positive controls (Aurora B and UBASH3B) (Figure 1A). UCHL3 belongs to the family of ubiquitin C-terminal hydrolases (UCH) containing also UCHL1, BRCA1-associated protein 1 (BAP1), and UCHL5. UCHL3 has been implicated in neurodegenerative disorders⁴⁰ and cancer^{41,42} but it has not been

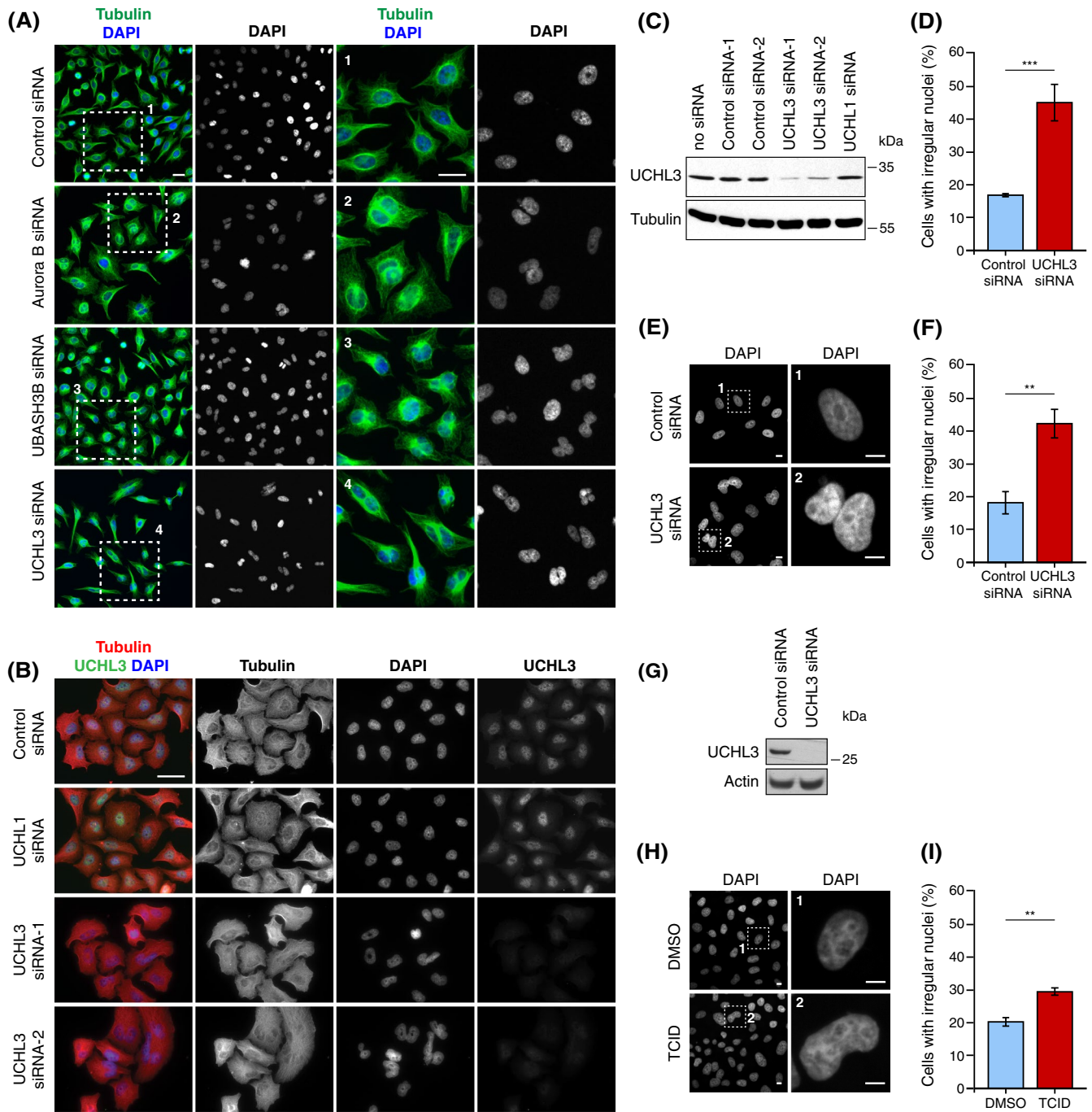
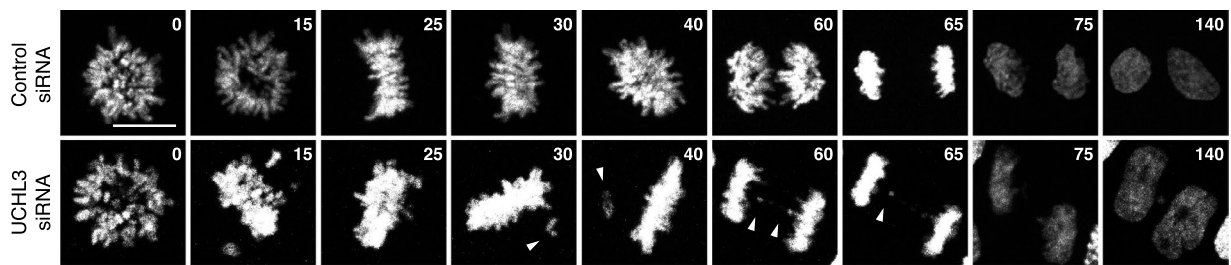


FIGURE 1 UCHL3 controls euploidy of human cells. A-D, UCHL3 was downregulated by specific siRNAs used in the secondary screen (Table S1), and a distinct siRNA targeting a 3'UTR region of UCHL3 gene (E-G). A, HeLa cells were treated with indicated siRNA pools and analyzed by immunofluorescence microscopy. The magnified regions are shown in the corresponding numbered panels. Scale bar 5 μ m. B-D, HeLa cells were transfected with single siRNAs as indicated and analyzed by immunofluorescence (B) and by western blotting (C). Scale bar 5 μ m. D, The percentage of cells with irregular nuclei was quantified, mean \pm SD of three experiments. Control = 16.4 ± 0.2 , UCHL3 siRNA-1 = 44.5 ± 5.3 , $P = .0008$. E-G, HeLa cells were treated with control and UCHL3 3'UTR siRNAs as indicated and analyzed by immunofluorescence (E). Scale bar 5 μ m. The magnified regions are shown in the corresponding numbered panels. Scale bar 2 μ m. F, Percentage of cells with irregular nuclei, mean of four experiments \pm SEM. Control = 18.3 ± 3.3 , $n = 886$ cells, UCHL3 3'UTR siRNA = 42.3 ± 4.3 , $n = 828$ cells, $P = .0043$. G, Western blot analysis confirming UCHL3 knockdown using UCHL3 3'UTR siRNAs. H-I, HeLa cells were treated with UCHL3 inhibitor (TCID) and analyzed by immunofluorescence microscopy (H). Scale bar 5 μ m. The magnified regions are shown in the corresponding numbered panels. Scale bar 2 μ m. I, Percentage of cells with irregular nuclei, mean of four experiments \pm SEM. Control (DMSO) = 19.5 ± 1.1 , $n = 2110$ cells, TCID = 28.6 ± 1.1 , $n = 2230$ cells, $P = .0012$.

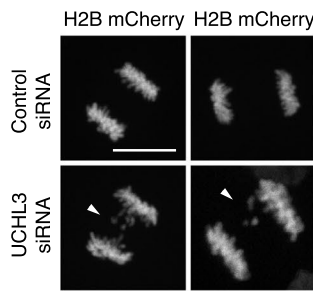
linked to the regulation of mitosis. To confirm its role in cell division, we downregulated UCHL3 by specific siRNAs used in the secondary screen (Table S1) (Figure 1B-D), and a distinct siRNA targeting a 3'UTR region of UCHL3 gene (Figure 1E-G). UCHL3 downregulation was confirmed by western blotting (Figure S1A) and by immunofluorescence microscopy using commercial UCHL3 antibody (Figure 1B), which revealed dispersed nuclear and cytoplasmic localization of UCHL3 in interphase cells. Western blotting using home-made, purified UCHL3 polyclonal antibody confirmed

the downregulation of UCHL3 (Figure 1G, Figure S1B). Immunofluorescence microscopy using home-made UCHL3 antibody demonstrated similar nuclear and cytoplasmic localization of UCHL3 (Figure S1C). A similar localization pattern could be also observed using overexpressed GFP-tagged UCHL3 (Figure S1D). In agreement with results obtained by the unbiased screening (Figure 1A), downregulation of UCHL3, but not UCHL1, led to a strong reduction in its protein levels (Figure 1B-G, Figure S1A, B) and markedly increased the number of cells with irregular, multilobed nuclei

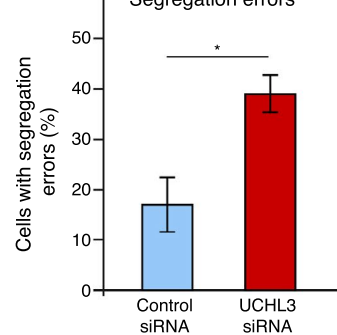
(A) Live video - HeLa Kyoto H2B mCherry (siRNA)



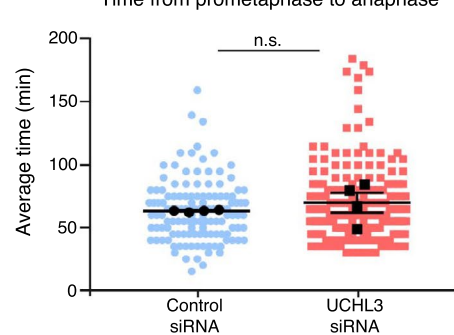
(B) H2B mCherry H2B mCherry



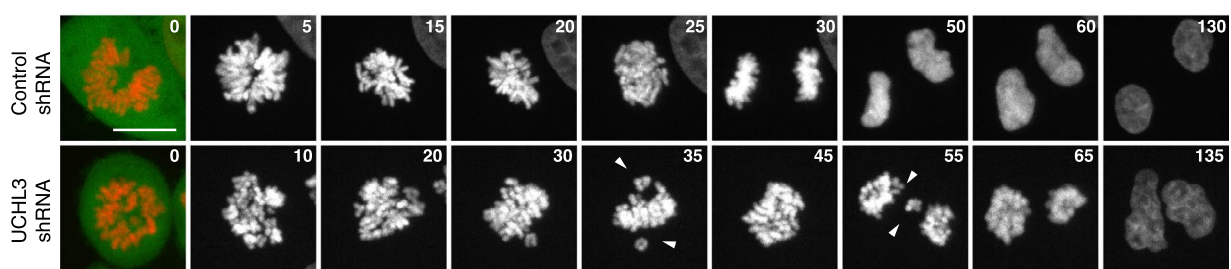
(C) Segregation errors



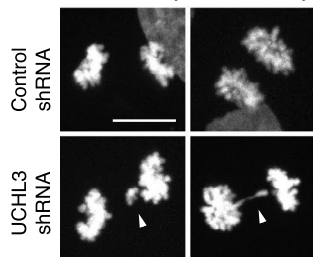
(D) Time from prometaphase to anaphase



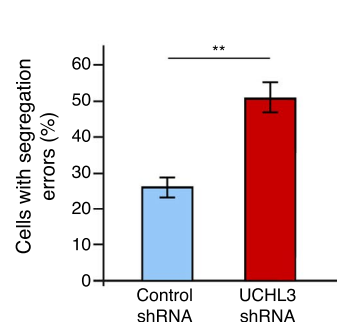
(E) Live video - Dld1 H2B mCherry (shRNA)



(F) H2B mCherry H2B mCherry



(G) Segregation errors



(H) Time from prometaphase to anaphase

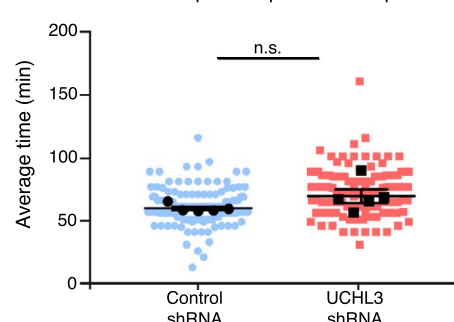


FIGURE 2 UCHL3 regulates chromosome segregation. A-D, HeLa cells stably expressing H2B-mCherry (DNA) were treated with siRNAs as indicated, synchronized in prometaphase and analyzed by video microscopy. $t = 0$ corresponds to the release from prometaphase block induced by monastrol. A, Selected time-frames show a DNA single channel (gray). Arrowheads point to misaligned chromosomes and segregation errors. Time is indicated in minutes. Scale bar 5 μm . B, Examples of observed segregation errors from A. Scale bar 5 μm . C, Percentage of cells with segregation errors from A, mean \pm SEM of four experiments. Control = 17.07 ± 5.92 , $n = 127$ cells, UCHL3 siRNA 39.01 ± 3.78 , $n = 198$ cells, $P = .0354$. D, Average time needed to proceed from prometaphase to anaphase, mean [min] \pm SEM of four experiments. Control = 63.8 ± 0.4 , UCHL3 siRNA = 70.4 ± 7.0 , $P = .4450$. Colored dots represent values of individual cells, black symbols represent the mean experimental value used for statistical analysis. E-H, Dld1-H2B-mCherry cells stably expressing GFP-shRNAs were synchronized in prometaphase and analyzed by live video microscopy (E) Selected time frames showing DNA channel (gray), $t = 0$ corresponds to the release from prometaphase block induced by monastrol, GFP-shRNA (green), DNA (red). Time is indicated in minutes. Scale bar 5 μm . F, Examples of observed segregation errors. Scale bar 5 μm . G, Percentage of cells with segregation errors, mean \pm SEM of five experiments. Control = 26.1 ± 3.2 , $n = 125$ cells, UCHL3 shRNA = 50.7 ± 5.4 , $n = 118$ cells, $P = .0069$. H, Average time needed to proceed from prometaphase to anaphase, mean [min] \pm SEM of five experiments. Control = 59.2 ± 1.2 , UCHL3 shRNA 68.7 ± 4.5 , $P = .1299$. Colored dots represent values of individual cells, black symbols represent the mean experimental value used for statistical analysis

(Figure 1B,D-F). Treatment with potent, cell permeable UCHL3-specific inhibitor 4,5,6,7-Tetrachloro-1*H*-Indene-1,3(2*H*)-dione (TCID) also resulted in the accumulation of cells with nuclear morphology defects (Figure 1H,I), suggesting that UCHL3 DUB activity might regulate faithful cell division.

3.2 | UCHL3 regulates chromosome segregation

To understand if and how UCHL3 regulates mitotic progression, we employed spinning disk live video microscopy of HeLa cells stably expressing histone marker H2B-mCherry, which were synchronized in prometaphase using the Eg5 inhibitor monastrol and released. This analysis showed that the downregulation of UCHL3 led to chromosome alignment defects in metaphase and to segregation errors in anaphase (Figure 2A-C). The live video microscopy analysis further revealed a minor delay in the time of mitotic progression from prometaphase to anaphase although the combined results from all experiments did not reach statistical significance (Figure 2D). The same results were obtained in the p53-negative DLD1 colorectal adenocarcinoma cell line stably expressing histone marker H2B-mCherry where shRNA-mediated downregulation of UCHL3 (Figure S2E) led to chromosome segregation defects but not to a statistically significant delay in anaphase onset (Figure 2E-H).

To exclude any indirect effects of monastrol usage, HeLa H2B-mCherry and DLD1 H2B-mCherry cell lines were synchronized in G1/S by a double thymidine block and release protocol and mitotic progression was analyzed using spinning disk confocal live imaging. Also under these experimental conditions, the downregulation of UCHL3 led to alignment and segregation defects in both cell lines without significantly affecting the time from nuclear envelope breakdown to anaphase (Figure S2A-D). Since the downregulation of UCHL3 does not lead to a severe mitotic arrest expected for a key mitotic component, we conclude that UCHL3 can

solely contribute to the regulation of faithful chromosome segregation in human cells.

In line with this assumption, CRISPR-CAS9-mediated knock-out cells of UCHL3 (Figure S2F), which were synchronized in G1/S by a double thymidine block and release protocol progressed normally through cell cycle relative to isogenic control cells as monitored by cyclin B accumulation and degradation (Figure S2F). In addition, we observed no differences in protein levels of the mitotic factors HOIP the subunit of the linear chain assembly E3 ligase LUBAC⁴³ and protein phosphatase 1 gamma (PP1 γ)⁴⁴ in UCHL3 knock-out cells synchronously progressing through cell cycle relative to controls (Figure S2F). Thus, UCHL3 is not an essential gene but may contribute to the regulation of chromosome segregation during mitosis. Chromosome segregation errors observed in UCHL3-deficient cells are likely to induce NoCut checkpoint and/or inhibit abscission and cytokinesis^{45,46} leading to irregular nuclei phenotype (Figure 1A,B,E,H).

3.3 | UCHL3 regulates chromosome bi-orientation

Since UCHL3 knock-out cells demonstrated biochemical characteristics of normal mitosis, and UCHL3 siRNA-treated cells displayed modest defects in mitotic progression, we next aimed to characterize in detail the chromosome alignment phenotype observed in UCHL3-deficient cells (Figure 2A,E, Figure S2A,B). First, we performed immunofluorescence microscopy on fixed cells to analyze kinetochore localization of the SAC protein BubR1. The downregulation of UCHL3 did not affect the localization of endogenous BubR1 to kinetochores in prometaphase (Figure S3A-C). In addition, protein levels of BubR1 and MAD2 were not changed throughout the cell cycle in the UCHL3 knock-out cells relative to controls (Figure S2F). Our results suggest that SAC remains functional in the absence of UCHL3.

To understand how UCHL3 contributes to the regulation of bi-orientation of chromosomes, we synchronized cells in

metaphase by monastrol block and release into proteasome inhibitor MG132 and fixed them before further analysis. Since proteasome-mediated degradation of securin and cyclin B is necessary for progression into anaphase, inhibition of 26S proteasome serves as an efficient way to synchronize cells in metaphase. The downregulation of UCHL3 led to an increase of metaphase cells with misaligned chromosomes often detected in the proximity of the spindle poles (Figure 3A,B). To understand if UCHL3 specifically regulates chromosome alignment to metaphase plate we performed rescue experiments, where 3'UTR directed siRNAs to the UCHL3 gene were simultaneously transfected with GFP-tagged wild type or catalytically inactive versions of UCHL3 (Figure 3C,D). Expression of wild-type, but not catalytically inactive UCHL3, partially rescued chromosome alignment defects upon the downregulation of UCHL3 (Figure 3C,E). These results suggest that UCHL3 specifically regulates chromosome bi-orientation in a manner that is dependent on its catalytic

activity. Similar chromosome alignment defects were also observed in UCHL3 knock-out cells (Figure 3F, Figure S6A). siRNA-mediated downregulation of Ku80 (Figure S4A), reported direct deubiquitylation substrate of UCHL3⁴⁷ and the core non-homologous end-joining (NHEJ) factor, did not result in defects in chromosome alignment as compared to UCHL3 siRNA and relative to control siRNA treated cells (Figure S4B,C). This observation suggests that mitosis-specific regulation of chromosome alignment by UCHL3 is likely not linked to Ku80 although any indirect effect of this factor to mitotic progression cannot be conclusively ruled out at this stage of analysis.

To further exclude the possibility that chromosome alignment errors observed in UCHL3-deficient cells are indirect due to possible defects in earlier cell cycle stages, we used UCHL3-specific inhibitor TCID, which led to the similar nuclear morphology defects as in UCHL3-downregulated cells (Figure 1H,I). We compared longer treatments where

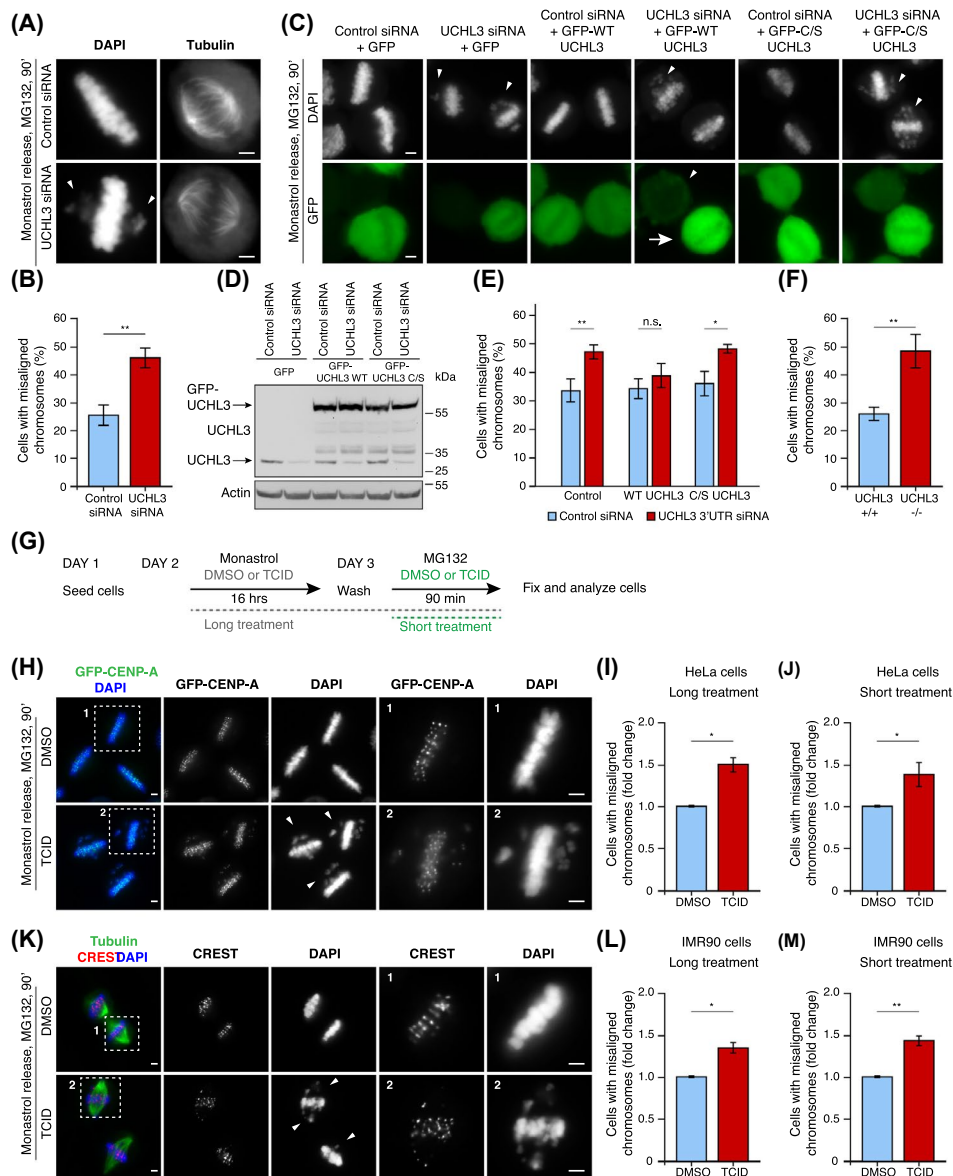


FIGURE 3 UCHL3 activity specifically regulates chromosome bi-orientation. A, B, HeLa cells were treated with indicated siRNAs, synchronized in metaphase, and analyzed by immunofluorescence microscopy. Arrowheads point to misaligned chromosomes. Scale bar 2 μ m. B, Percentage of cells with at least one misaligned chromosome, mean \pm SEM of seven experiments. Control = 25.2 ± 3.7 , $n = 2356$ cells, UCHL3 3'UTR siRNA = 45.4 ± 4.2 , $n = 2801$ cells, $P = .0034$. C-E, HeLa cells co-transfected with siRNAs as indicated and GFP, GFP-WT-UCHL3 (wild type), GFP-C/S-UCHL3 (catalytic dead) constructs were synchronized to metaphase, and analyzed by immunofluorescence microscopy (C). Arrowheads point to the misaligned chromosomes. Note: UCHL3 siRNA-treated cells expressing a low level of UCHL3-GFP-WT (arrowhead in the GFP channel) do not show rescue of the misalignment phenotype, while cells expressing a high level of UCHL3-GFP-WT (arrow) do. Scale bar 2 μ m. D, UCHL3 knockdown efficiency and expression of the GFP-forms of UCHL3 were analyzed on the same membrane by western blotting with antibodies against UCHL3 and Actin. Positions of the endogenous and GFP-tagged UCHL3 proteins are indicated. E, Percentage of cells shown in C with misaligned chromosomes was quantified for each category, mean \pm SEM of four experiments, 37.3 ± 2.5 , 46.2 ± 1.7 , 37.5 ± 2.6 , 40.9 ± 3.0 , 39.0 ± 2.7 , 46.7 ± 0.9 with total number of cells analyzed: 1670, 2632, 1943, 2088, 2266, 2149 and P values $P = .0242$, $P = .4306$, $P = .0366$, respectively. F, UCHL3 wild type (UCHL3+/+) and knockout (UCHL3-/-) HeLa cells were synchronized in metaphase and the percentage of misaligned chromosomes was quantified, mean \pm SD of three experiments, UCHL3+/+ = 23.9 ± 2.5 , UCHL3-/- = 47.6 ± 6.0 , $P = .0033$. G, A scheme of the synchronization protocol used for "long treatment" (gray) and "short treatment" (green) with the UCHL3 inhibitor TCID. H-J, HeLa cells stably expressing GFP-CENP-A were synchronized by long-term treatment protocol described in G and analyzed by immunofluorescence microscopy (H). Magnified regions are shown in the corresponding numbered panels. Arrowheads point to misaligned chromosomes. Scale bar 2 μ m. I, Cells with misaligned chromosomes were quantified, shown as fold change, mean \pm SEM of three experiments. Control (DMSO) = 1, $n = 830$ cells, TCID = 1.50 ± 0.06 , $n = 1090$ cells, $P = .0157$. J, Quantification of misaligned chromosomes in short-term treatment shown as the fold increase, mean \pm SEM of four experiments. Control (DMSO) = 1.0, $n = 1260$ cells, TCID = 1.39 ± 0.13 , $n = 1541$ cells, $P = .0394$. K-M, Human primary fibroblasts (IMR90) were analyzed as described in H. Magnified regions are shown in the corresponding numbered panels (K). Arrowheads point to misaligned chromosomes. Scale bar 2 μ m. L, Cells with misaligned chromosomes after the long-term treatment were quantified, shown as a fold change, mean \pm SEM of three experiments. Control (DMSO) = 1, $n = 1378$ cells, TCID = 1.34 ± 0.07 , $n = 1571$ cells, $P = .0190$. M, Quantification of cells with misaligned chromosomes after the short-term treatment shown as the fold increase, mean \pm SEM of five experiments. Control (DMSO) = 1.0, $n = 951$ cells, TCID = 1.43 ± 0.06 , $n = 994$ cells, $P = .0055$

the inhibitor was used simultaneously with monastrol for 16 hours and after the release into MG132 to allow for the formation of metaphase plates with the shorter treatments where TCID was only administered after monastrol release into MG132 (Figure 3G). Importantly, the results from long (Figure 3H,I) and short (Figure 3J) TCID treatments were almost indistinguishable and both experimental conditions led to the accumulation of misaligned polar chromosomes relative to solvent control. Importantly, the same results were obtained in human primary lung fibroblasts IMR-90 (Figure 3K-M), suggesting a similar mitotic role of UCHL3 in non-transformed cells. Thus, UCHL3 activity may specifically contribute to the regulation of chromosome bi-orientation as cells progressively form the metaphase plate.

To understand if UCHL3 is involved in the formation of MT-KT attachments, we performed confocal immunofluorescence microscopy on fixed metaphase cells (Figure 4A). In line with the earlier experiments (Figure 3A,C,H,K), we frequently observed the sister kinetochore pairs, which partially or completely lacked direct contacts with microtubules upon the downregulation of UCHL3 (Figure 4A). Next, we analyzed kinetochore localization of astrin, the marker of stable amphitelic attachments in metaphase-synchronized cells. The downregulation of UCHL3 slightly reduced the recruitment of astrin to kinetochores on centered chromosomes located in the proximity to the metaphase plate as well as on polar chromosomes located closer to the spindle poles (Figure 4B-D) relative to control cells, suggesting that UCHL3 may be involved, to a certain extent, in the formation

of proper MT-KT attachments. Taken together, our observations suggest that UCHL3 specifically contributes to chromosome bi-orientation during the transition from prometaphase to metaphase possibly by regulating the formation of correct MT-KT attachments.

3.4 | UCHL3 interacts with and deubiquitylates Aurora B and promotes its localization to kinetochores

We hypothesized that UCHL3 acts on Aurora B, one of the major factors driving chromosome bi-orientation and segregation during mitosis. Western blotting analysis of UCHL3 knock-out cells revealed no differences in total protein levels of Aurora B (Figure 5A,B). No differences in protein levels of cyclin B, PP1 γ , and CENP-E were observed in the absence of UCHL3 relative to control cells during progression through prometaphase (Figure 5B). No changes in protein levels of Aurora B were also observed in UCHL3 knock-out cells released from G1-arrest synchronously progressing through cell cycle relative to controls (Figure S2F). Moreover, immunoprecipitated wild-type UCHL3-GFP and catalytically dead UCHL3-GFP interacted with endogenous Aurora B and with ubiquitin (Figure 5C) in prometaphase cells, suggesting that UCHL3 may bind to polyubiquitin-modified forms of Aurora B. Immunoprecipitation of GFP-Aurora B under denaturing conditions confirmed the existence of polyubiquitin-modified forms of Aurora B in prometaphase

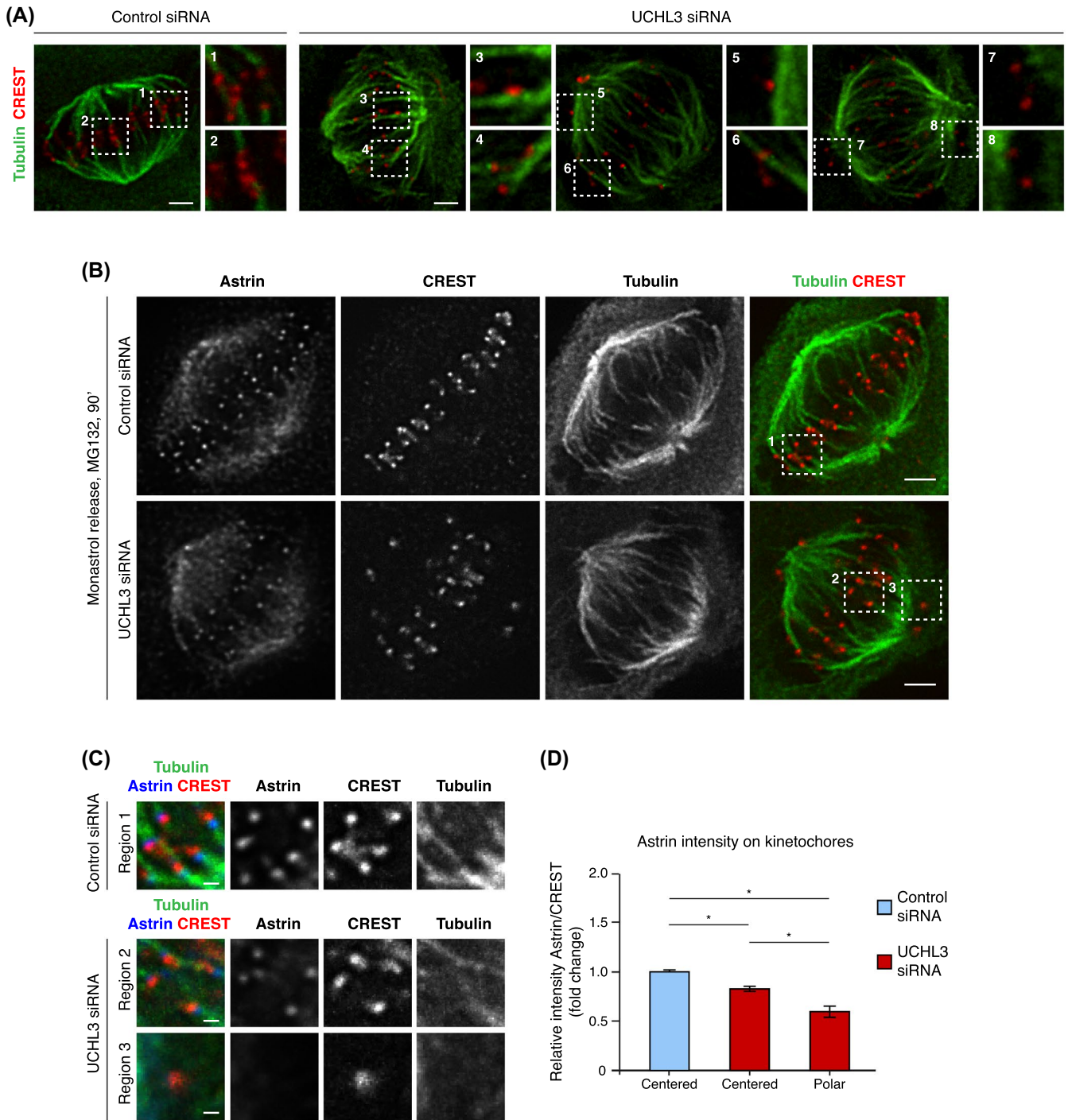


FIGURE 4 UCHL3 is required for the formation of stable MT-KT attachments. A, HeLa cells were treated with siRNAs as indicated, synchronized in metaphase, and analyzed by immunofluorescence microscopy. Magnified regions are shown in the corresponding numbered panels. Scale bar 2 μ m. B-D, HeLa cells were treated and synchronized as in A and analyzed by immunofluorescence microscopy (B). Magnified regions are shown in the corresponding numbered panels in C. Scale bar 0.5 μ m. D, Relative astrin intensity (astrin/CREST ratio) on kinetochores of centered and polar chromosomes was quantified and is shown as a fold change to control condition. Results are presented as mean \pm SD of four experiments. Control siRNA = 1, n = 4017 kinetochores, UCHL3 siRNA Centered = 0.82 ± 0.06 , n = 3962 kinetochores, UCHL3 siRNA Polar = 0.59 ± 0.07 , n = 470 kinetochores, P values: Control siRNA to UCHL3 siRNA Centered P = .0114, Control siRNA to UCHL3 siRNA Polar P = .0107, UCHL3 siRNA Centered to UCHL3 siRNA Polar P = .0244

cells (Figure 5D). Interestingly, in the UCHL3 knock-out cells strong increase of polyubiquitin modification on immunoprecipitated GFP-Aurora B was observed (Figure 5D).

These results are consistent with the possibility that UCHL3 deubiquitylates Aurora B in prometaphase cells to regulate its function in chromosome bi-orientation and segregation.

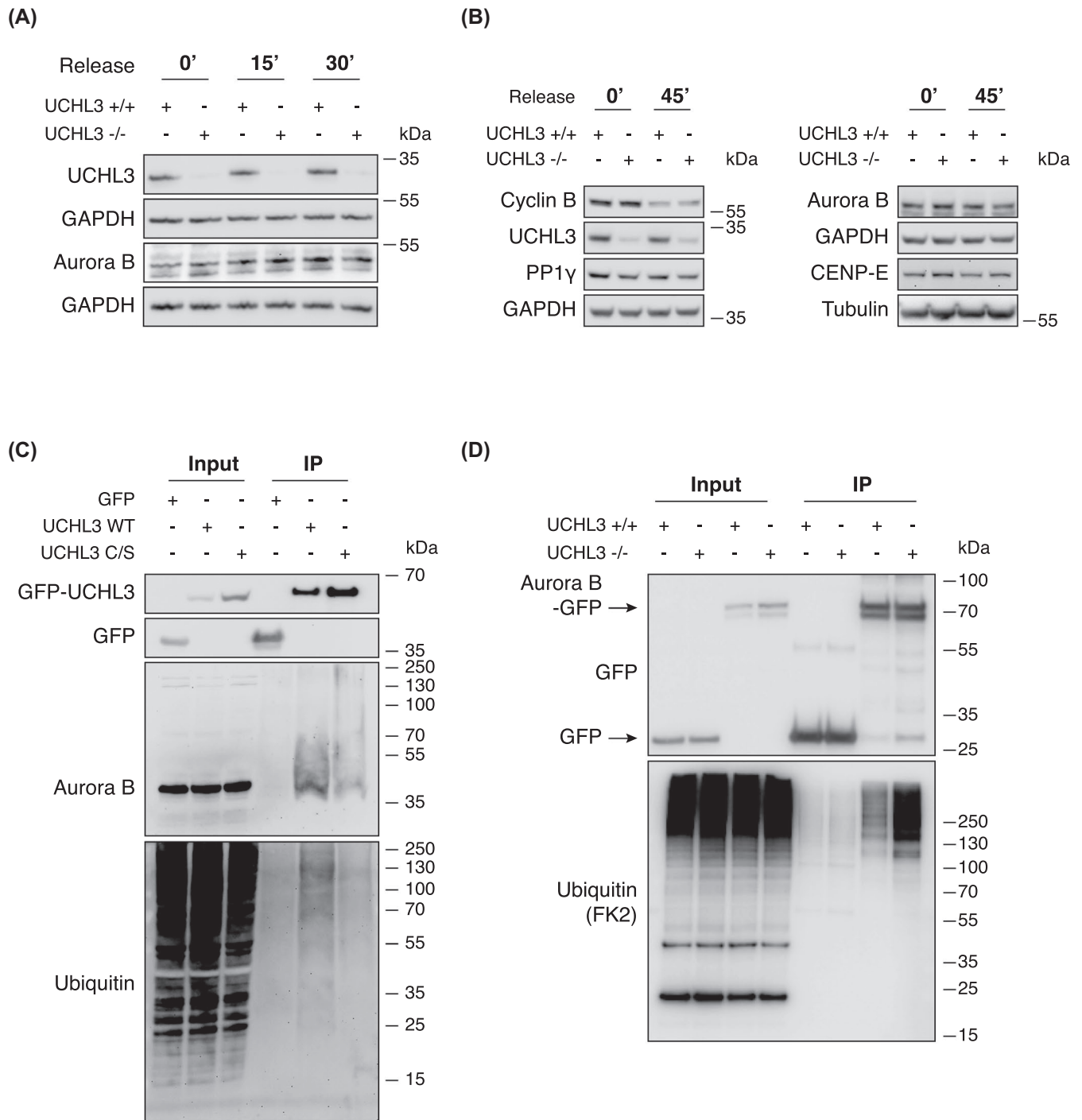


FIGURE 5 UCHL3 interacts with and deubiquitylates Aurora B in mitotic cells. A, B, Clonally selected UCHL3^{+/+} and UCHL3^{-/-} HeLa cells were synchronized in prometaphase by monastrol (0'), released into fresh medium for 15, 30 minutes (') (A) or 45 minutes (B) and analyzed by western blotting. C, HeLa cells stably expressing, GFP, GFP-UCHL3-WT (wild type) or GFP-UCHL3-C/S (catalytic dead) constructs were synchronized in prometaphase by STLC and the lysates were immunoprecipitated (IP) with GFP-Trap beads and analyzed by western blotting. D, UCHL3^{+/+} and UCHL3^{-/-} HeLa cells were transfected with Aurora B-GFP plasmid, synchronized in prometaphase by monastrol, immunoprecipitated with GFP-Trap beads under denaturing conditions and analyzed by western blotting. Membranes were probed with GFP and FK2 antibody recognizing the conjugated form of ubiquitin. Positions of GFP and GFP-tagged Aurora B proteins are indicated

Since UCHL3 does not regulate protein levels or degradation of Aurora B (Figure 5A,B and Figure S2F), we next aimed at understanding possible molecular outcomes of UCHL3-mediated regulation of Aurora B. Ubiquitylation of Aurora B

has been implicated in the regulation of its localization to mitotic structures,³¹⁻³⁵ we, therefore, first used HeLa knock-in cell line with endogenous Aurora B tagged with GFP tag and quantified the chromosomal intensities of Aurora B using

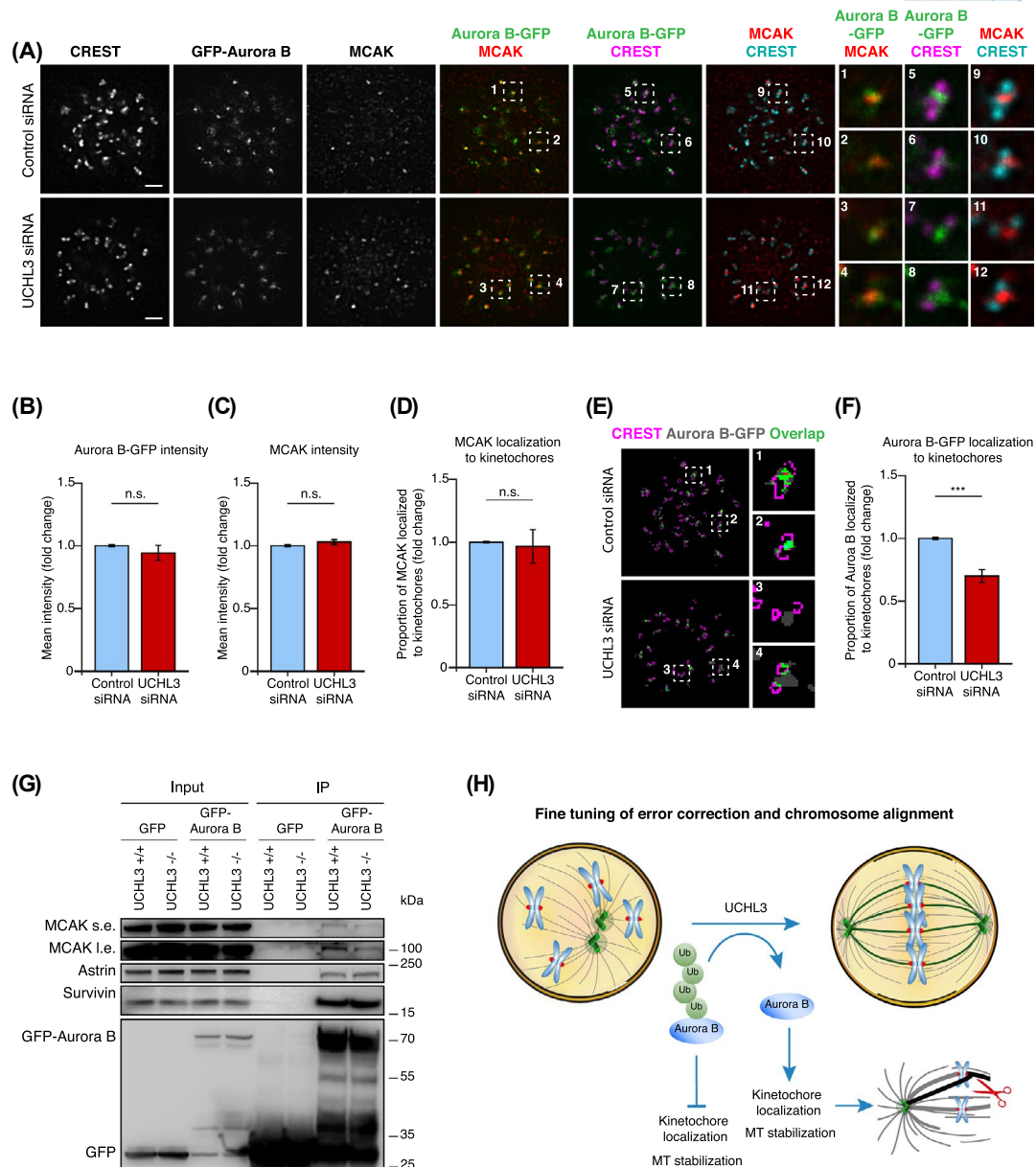


FIGURE 6 UCHL3 may promote localization of Aurora B to kinetochores. A-F, HeLa knock-in cells expressing GFP-tagged version of endogenous Aurora B were treated with siRNAs as indicated, synchronized in prometaphase, and analyzed by immunofluorescence microscopy with antibodies against MCAK and CREST. Maximum intensity projections are shown (A). Scale bar 2 μ m. Right: Magnified regions corresponding to numbered boxes. Representative examples of selected objects and intensity masks used for CellProfiler quantifications in the corresponding pictures are shown in Figure S5. B, Mean Aurora B intensity was quantified from single Z sections and normalized to control siRNA condition, mean of five experiments \pm SEM. Control = 1, n = 88 cells, UCHL3 siRNA = 0.946 \pm 0.054, n = 115 cells, P = .3775. C, Mean MCAK intensity from single Z sections was quantified and normalized to control siRNA condition, mean of three experiments \pm SEM. Control = 1, n = 73 cells, UCHL3 siRNA = 1.027 \pm 0.024, n = 100 cells, P = .4967. D, The fraction of MCAK signal on kinetochores normalized to control siRNA condition, mean of three experiments \pm SEM. Control = 1, n = 4944 kinetochores, UCHL3 siRNA = 0.95 \pm 0.05, n = 5460 kinetochores, P = .4992. E and F, Cells from A were analyzed by immunofluorescence microscopy and by CellProfiler software. Kinetochore objects (pink), Aurora B objects (gray), overlapping regions (green) are shown. F, CellProfiler-based quantifications of the fraction of Aurora B signal overlapping with kinetochores normalized to control siRNA condition. G, UCHL3^{+/+} and UCHL3^{-/-} HeLa cells were transfected with Aurora B-GFP plasmid, synchronized by monastrol, immunoprecipitated with GFP-Trap beads and analyzed by western blotting. The panel shows a representative result of three independent experiments. H, A hypothetical model of how UCHL3 contributes to the regulation of chromosome alignment and segregation. Despite being a non-essential gene, the UCHL3 function in mitosis may be specifically required for the deubiquitylation of Aurora B in prometaphase. This event is necessary for proper Aurora B localization to kinetochores and its function in the correction of erroneous MT-KT attachments possibly through regulation of MCAK. UCHL3 may, therefore, promote microtubule stabilization and fine-tuning of the error correction machinery as cells progressively form the metaphase plate. Polyubiquitylated Aurora B cannot localize to kinetochores, resulting in microtubule destabilization, and alignment and segregation errors. Green circle (Ub) = ubiquitin, blue oval = Aurora B kinase

CellProfiler-based automated image analysis (Figure 6A, Figure S5A). The number of Aurora B positive objects (Figure S5B), objects areas (Figure S5C), and the mean intensity of Aurora B signal were unchanged in UCHL3-downregulated cells relative to control cells (Figure 6A,B). Similarly, the integrated intensity of endogenous Aurora B was comparable in UCHL3 knock-out cells and isogenic controls (Figure S6A,B), and UCHL3 knock-out cells displayed chromosome alignment defects (Figure S6A) as expected. Analysis of intensity and kinetochore localization of MCAK, one of the main error correction factors and direct substrates of Aurora B,^{15,18} in UCHL3 deficient cells revealed no differences relative to control cells (Figure 6A,C,D, Figure S5D-F), despite a reduction in the number of CellProfiler-identified MCAK objects (Figure S5E). The number of CREST antibody-positive kinetochore objects detected by the software (Figure S5G,H) and the mean intensity of CREST signal (Figure S5I) was unchanged in UCHL3 deficient cells relative to controls. Interestingly, the proportion of Aurora B localized to kinetochores in UCHL3-downregulated cells was reduced relative to control siRNA-treated cells (Figure 6E,F). The analysis of the interaction of immunoprecipitated GFP wild-type Aurora B with MCAK showed a minor decrease in binding in UCHL3 knock-out cells relative to control cells, while the binding of Aurora B to the CPC component survivin and the kinetochore factor astrin remained unchanged in UCHL3 knock-out cells (Figure 6G). These results suggest that UCHL3 activity promotes localization of Aurora B to kinetochores to fine-tune the levels of this kinase required for correction of misaligned chromosomes as cells progress from prometaphase to metaphase.

4 | DISCUSSION

Taken together, our data suggest a model (Figure 6H) how UCHL3-mediated deubiquitylation maintains euploidy in human cells. UCHL3-deficient cells display defects in the bi-orientation of chromosomes at the mitotic spindle during metaphase (Figure 3A-F) and frequent errors in chromosome segregation during anaphase (Figure 2A-C,E-G, and Figure S2A,B). It is probable that nuclear morphology defects observed in the absence of UCHL3 activity (Figure 1A,B,D-F,H,I) result from an abscission block caused by lagging chromosomes during anaphase.^{45,46} It would be interesting to know if the lagging chromosomes observed during anaphase of UCHL3-deficient cells correspond to the same chromosomes which failed to align at the metaphase plate, which currently cannot be answered based on available evidence.

Our data suggest that in the absence of UCHL3 chromosomes with incorrect MT-KT attachments accumulate at the transition from prometaphase to metaphase (Figure 3H-M,

Figure 4A) where kinetochore localization of astrin, a marker of stable MT-KT attachment (Figure 4B-D) is moderately perturbed. Our results suggest that UCHL3 specifically regulates the alignment of chromosomes as cells progress from prometaphase to metaphase, despite being a non-essential gene. First, the alignment defects observed upon UCHL3 downregulation by siRNA can be partially rescued by expression of WT but not catalytically inactive form of UCHL3 (Figure 3C-E). Similarly, CRISPR-CAS9-mediated UCHL3 knock-out cells display unaligned polar chromosomes in metaphase relative to controls (Figure 3F, Figure S6A). In addition to HeLa cells, the alignment defects can also be observed in UCHL3-deficient p53-negative DLD1 cells (Figure 2E, Figure S2B) and in human primary lung fibroblasts IMR-90 (Figure 3K-M), suggesting a similar mitotic role of UCHL3 in non-transformed cells. The observed alignment defects are likely not due to misregulation of DNA repair by the NHEJ factor Ku80, a direct deubiquitylation substrate of UCHL3,⁴⁷ as Ku80-downregulated cells display no differences in the number of misaligned chromosomes relative to control cells in contrast to UCHL3-downregulated cells (Figure S4A-C) although any indirect effect of Ku80 to mitotic progression cannot be conclusively ruled out at this stage of analysis. Finally, the use of UCHL3-specific inhibitor TCID for a short period during prometaphase led to the accumulation of misaligned polar chromosomes relative to solvent control, a defect almost indistinguishable from longer TCID treatments (Figure 3H-M). Thus, UCHL3 activity might be specifically required for the correction of improperly aligned chromosomes as cells progressively form the metaphase plate.

Several lines of observations suggest that UCHL3 may directly regulate the function of Aurora B, one of the main factors driving the fidelity of MT-KT attachments and chromosome bi-orientation and segregation.^{7,8,10-12} First, UCHL3 interacts with Aurora B during prometaphase (Figure 5C). Furthermore, immunoprecipitations under denaturing conditions reveal the presence of polyubiquitylated form of Aurora B in the prometaphase cells, a modification that accumulates in the absence of UCHL3 (Figure 5D). Finally, UCHL3 DUB activity seems required for the role of UCHL3 in chromosome bi-orientation (Figure 3C-E). Together, these results are consistent with the possibility that UCHL3 directly deubiquitylates polyubiquitylated Aurora B during prometaphase. It is unlikely that UCHL3-mediated deubiquitylation regulates proteolysis of Aurora B as the protein levels of Aurora B remain unchanged through mitotic progression in the absence of UCHL3 (Figure 5A, B, Figure S2F). Previous findings demonstrated the role of CUL3-mediated monoubiquitylation of Aurora B³¹⁻³⁴ recognized by the ubiquitin-binding protein UBASH3B^{35,48} in the localization of this kinase to centromeres and microtubules. However, the absence of UCHL3

led to an increase in polyubiquitylation and not monoubiquitylation signals on Aurora B (Figure 5D). Moreover, the levels of NEDD8-modified CUL3 remained unchanged in the absence of UCHL3 (data not shown), excluding the possibility that UCHL3 indirectly affects the activity of CUL3, which could be anticipated based on previously reported dual deubiquitylating and deneddylating activity of UCHL3.^{49,50} While future experiments will have to identify UCHL3-sensitive-specific linkage type of polyubiquitin chains detected on Aurora B, it is unlikely that UCHL3 acts in the CUL3-UBASH3B signaling axis and in the APC/C-mediated proteolysis of Aurora B.

Instead, our findings suggest that one possible molecular consequence of the increase in Aurora B polyubiquitylation in the absence of UCHL3 is a reduction in the localization of Aurora B to kinetochores (Figure 6E,F). We also observed a minor decrease in the interaction of Aurora B with MCAK but not with other Aurora B-binding partners such as astrin and the CPC component survivin (Figure 6G). MCAK activity as a microtubule depolymerase on incorrectly formed MT-KT attachments is inhibited by direct Aurora B-mediated phosphorylation¹⁴⁻²⁰ and deletion of MCAK leads to the increased number of laterally attached kinetochores resulting in bi-orientation defects and segregation errors.¹⁷ We speculate, that UCHL3-driven deubiquitylation of Aurora B promotes its localization to kinetochores and may affect interaction with MCAK allowing in turn for stabilization of MT-KT attachments as cells progressively form the metaphase plate (Figure 6H). This fast and reversible mechanism would allow for the fine-tuning of error correction machinery during prometaphase progression. While future studies are needed to understand the identity of the E3-ubiquitin ligase able to catalyze the UCHL3-sensitive Aurora B polyubiquitylation, our findings not only expand our knowledge on the ubiquitin-mediated regulation of Aurora B localization during mitosis but also fill up the knowledge gap on the specific mitotic roles of human deubiquitylases. Since UCHL3 has been recently implicated in human cancer,^{32,33} our data may open interesting perspectives for studying the role of this DUB in the carcinogenesis process.

ACKNOWLEDGMENTS

We thank Snezhana Oliferenko, Manuel Mendoza, Bill Keyes, and the members of the Sumara group for helpful discussions on the manuscript. Kallayane Chawengsaksophak for mentorship and support. We are grateful to Don Cleveland, Ulrike Gruneberg, and Jason Swedlow for help with reagents. We thank the Imaging Center of the IGBMC (ICI) for help on confocal microscopy and to the IGBMC core facilities for their support on this research. KJ was supported by a fellowship from Gouvernement français et L'Institut français de Prague,

Charles University, Prague, a LabEx international PhD fellowship from IGBMC and a fellowship from the "Ligue Nationale Contre le Cancer". YL is supported by a PhD fellowship from the China Scholarship Council (CSC). Research in RS laboratory was supported by funding from The Czech Academy of Sciences (RVO68378050) and from the Czech Centre for Phenogenomics by the Ministry of Education, Youth, and Sports of the Czech Republic (LM2015040). This study was supported by the grant ANR-10-LABX-0030-INRT, a French State fund managed by the Agence Nationale de la Recherche under the frame program Investissements d'Avenir ANR-10-IDEX-0002-02. Research in IS laboratory was supported by IGBMC, CNRS, Fondation ARC pour la recherche sur le cancer, Institut National du Cancer (INCa), Agence Nationale de la Recherche (ANR), Ligue Nationale contre le Cancer, USIAS, Programme Fédérateur Aviesan from INSERM and Sanofi iAward Europe.

CONFLICT OF INTEREST

The authors declare no competing financial interests.

AUTHOR CONTRIBUTIONS

K. Jerabkova and Y. Liao designed and performed experiments and helped to write the manuscript. C. Kleiss, S. Fournane, M. Durik, and A. Agote-Arán helped to perform experiments. L. Brino helped to design and perform the siRNA screens. R. Sedlacek helped to design the experiments and to supervise the project. I. Sumara supervised the project, designed the experiments, and wrote the manuscript with input from all authors.

REFERENCES

1. Ben-David U, Amon A. Context is everything: aneuploidy in cancer. *Nat Rev Genet.* 2020;21(1):44-62.
2. Musacchio A. Spindle assembly checkpoint: the third decade. *Philos Trans R Soc Lond B Biol Sci.* 2011;366:3595-3604.
3. Musacchio A, Salmon ED. The spindle-assembly checkpoint in space and time. *Nat Rev Mol Cell Biol.* 2007;8:379-393.
4. Musacchio A. The molecular biology of spindle assembly checkpoint signaling dynamics. *Curr Biol.* 2015;25:R1002-R1018.
5. Peters JM. The anaphase promoting complex/cyclosome: a machine designed to destroy. *Nat Rev Mol Cell Biol.* 2006;7:644-656.
6. Tanaka TU. Kinetochores-microtubule interactions: steps towards bi-orientation. *EMBO J.* 2010;29:4070-4082.
7. Biggins S, Murray AW. The budding yeast protein kinase Ipl1/Aurora allows the absence of tension to activate the spindle checkpoint. *Genes Dev.* 2001;15:3118-3129.
8. Tanaka TU, Rachidi N, Janke C, et al. Evidence that the Ipl1-Sli15 (Aurora kinase-INCENP) complex promotes chromosome bi-orientation by altering kinetochore-spindle pole connections. *Cell.* 2002;108:317-329.
9. Carmena M, Wheelock M, Funabiki H, Earnshaw WC. The chromosomal passenger complex (CPC): from easy rider to the godfather of mitosis. *Nat Rev Mol Cell Biol.* 2012;13:789-803.

10. Hauf S, Cole RW, LaTerra S, et al. The small molecule Hesperadin reveals a role for Aurora B in correcting kinetochore-microtubule attachment and in maintaining the spindle assembly checkpoint. *J Cell Biol.* 2003;161:281-294.
11. Ditchfield C, Johnson VL, Tighe A, et al. Aurora B couples chromosome alignment with anaphase by targeting BubR1, Mad2, and Cenp-E to kinetochores. *J Cell Biol.* 2003;161:267-280.
12. Kallio MJ, McClelland ML, Stukenberg PT, Gorbisky GJ. Inhibition of Aurora B kinase blocks chromosome segregation, overrides the spindle checkpoint, and perturbs microtubule dynamics in mitosis. *Curr Biol.* 2002;12:900-905.
13. Lampson MA, Cheeseman IM. Sensing centromere tension: Aurora B and the regulation of kinetochore function. *Trends Cell Biol.* 2011;21:133-140.
14. Knowlton AL, Lan W, Stukenberg PT. Aurora B is enriched at merotelic attachment sites, where it regulates MCAK. *Curr Biol.* 2006;16:1705-1710.
15. Andrews PD, Ovechkina Y, Morrice N, et al. Aurora B regulates MCAK at the mitotic centromere. *Dev Cell.* 2004;6:253-268.
16. Ems-McClung SC, Hainline SG, Devare J, et al. Aurora B inhibits MCAK activity through a phosphoconformational switch that reduces microtubule association. *Curr Biol.* 2013;23:2491-2499.
17. Kline-Smith SL, Khodjakov A, Hergert P, Walczak CE. Depletion of centromeric MCAK leads to chromosome congression and segregation defects due to improper kinetochore attachments. *Mol Biol Cell.* 2004;15:1146-1159.
18. Lan W, Zhang X, Kline-Smith SL, et al. Aurora B phosphorylates centromeric MCAK and regulates its localization and microtubule depolymerization activity. *Curr Biol.* 2004;14:273-286.
19. Wordeman L, Wagenbach M, von Dassow G. MCAK facilitates chromosome movement by promoting kinetochore microtubule turnover. *J Cell Biol.* 2007;179:869-879.
20. Zhang X, Lan W, Ems-McClung SC, Stukenberg PT, Walczak CE. Aurora B phosphorylates multiple sites on mitotic centromere-associated kinesin to spatially and temporally regulate its function. *Mol Biol Cell.* 2007;18:3264-3276.
21. Kim Y, Holland AJ, Lan W, Cleveland DW. Aurora kinases and protein phosphatase 1 mediate chromosome congression through regulation of CENP-E. *Cell.* 2010;142:444-455.
22. Schmidt JC, Kiyomitsu T, Hori T, Backer CB, Fukagawa T, Cheeseman IM. Aurora B kinase controls the targeting of the Astrin-SKAP complex to bioriented kinetochores. *J Cell Biol.* 2010;191:269-280.
23. Shrestha RL, Conti D, Tamura N, et al. Aurora-B kinase pathway controls the lateral to end-on conversion of kinetochore-microtubule attachments in human cells. *Nat Commun.* 2017;8:150.
24. Pinsky BA, Kung C, Shokat KM, Biggins S. The Ipl1-Aurora protein kinase activates the spindle checkpoint by creating unattached kinetochores. *Nat Cell Biol.* 2006;8:78-83.
25. Pinsky BA, Biggins S. The spindle checkpoint: tension versus attachment. *Trends Cell Biol.* 2005;15:486-493.
26. Krenn V, Musacchio A. The Aurora B kinase in chromosome bi-orientation and spindle checkpoint signaling. *Front Oncol.* 2015;5:225.
27. Santaguida S, Vernieri C, Villa F, Ciliberto A, Musacchio A. Evidence that Aurora B is implicated in spindle checkpoint signalling independently of error correction. *EMBO J.* 2011;30:1508-1519.
28. Saurin AT, van der Waal MS, Medema RH, Lens SMA, Kops GJPL. Aurora B potentiates Mps1 activation to ensure rapid checkpoint establishment at the onset of mitosis. *Nat Commun.* 2011;2:316.
29. Vader G, Crujnsen CWA, van Harn T, Vromans MJM, Medema RH, Lens SMA. The chromosomal passenger complex controls spindle checkpoint function independent from its role in correcting microtubule kinetochore interactions. *Mol Biol Cell.* 2007;18:4553-4564.
30. Lindon C, Pines J. Ordered proteolysis in anaphase inactivates Plk1 to contribute to proper mitotic exit in human cells. *J Cell Biol.* 2004;164:233-241.
31. Sumara I, Quadroni M, Frei C, et al. A Cul3-based E3 ligase removes Aurora B from mitotic chromosomes, regulating mitotic progression and completion of cytokinesis in human cells. *Dev Cell.* 2007;12:887-900.
32. Sumara I, Peter M. A Cul3-Based E3 ligase regulates mitosis and is required to maintain the spindle assembly checkpoint in human cells. *Cell Cycle.* 2007;6:3004-3010.
33. Maerki S, Olma MH, Staubli T, et al. The Cul3-KLHL21 E3 ubiquitin ligase targets Aurora B to midzone microtubules in anaphase and is required for cytokinesis. *J Cell Biol.* 2009;187:791-800.
34. Maerki S, Beck J, Sumara I, Peter M. Finding the midzone: the role of ubiquitination for CPC localization during anaphase. *Cell Cycle.* 2010;9:2921-2922.
35. Krupina K, Kleiss C, Metzger T, et al. Ubiquitin receptor protein UBASH3B drives Aurora B recruitment to mitotic microtubules. *Dev Cell.* 2016;36:63-78.
36. Fournane S, Krupina K, Kleiss C, Sumara I. Decoding ubiquitin for mitosis. *Genes Cancer.* 2012;3:697-711.
37. Jerabkova K, Sumara I. Cullin 3, a cellular scripter of the non-proteolytic ubiquitin code. *Semin Cell Dev Biol.* 2019;93:100-110.
38. Sumara I, Maerki S, Peter M. E3 ubiquitin ligases and mitosis: embracing the complexity. *Trends Cell Biol.* 2008;18:84-94.
39. Holland AJ, Fachinetti D, Han JS, Cleveland DW. Inducible, reversible system for the rapid and complete degradation of proteins in mammalian cells. *Proc Natl Acad Sci U S A.* 2012;109:E3350-E3357.
40. Dennissen FJA, Kholod N, Hermes DJHP, et al. Mutant ubiquitin (UBB+1) associated with neurodegenerative disorders is hydrolyzed by ubiquitin C-terminal hydrolase L3 (UCH-L3). *FEBS Lett.* 2011;585:2568-2574.
41. Song Z, Tu X, Zhou Q, et al. A novel UCHL3 inhibitor, perifosine, enhances PARP inhibitor cytotoxicity through inhibition of homologous recombination-mediated DNA double strand break repair. *Cell Death Dis.* 2019;10:398.
42. Zhang M-H, Zhang H-H, Du X-H, et al. UCHL3 promotes ovarian cancer progression by stabilizing TRAF2 to activate the NF- κ B pathway. *Oncogene.* 2020;39(2):322-333.
43. Wu M, Chang Y, Hu H, et al. LUBAC controls chromosome alignment by targeting CENP-E to attached kinetochores. *Nat Commun.* 2019;10:273.
44. Saurin AT. Kinase and phosphatase cross-talk at the kinetochore. *Front Cell Dev Biol.* 2018;6:62.
45. Norden C, Mendoza M, Dobbelaere J, Kotwaliwale CV, Biggins S, Barral Y. The NoCut pathway links completion of cytokinesis to spindle midzone function to prevent chromosome breakage. *Cell.* 2006;125:85-98.
46. Steigemann P, Wurzenberger C, Schmitz MH, et al. Aurora B-mediated abscission checkpoint protects against tetraploidization. *Cell.* 2009;136:473-484.

47. Nishi R, Wijnhoven PWG, Kimura Y, et al. The deubiquitylating enzyme UCHL3 regulates Ku80 retention at sites of DNA damage. *Sci Rep.* 2018;8:17891.
48. Krupina K, Kleiss C, Awal S, Rodriguez-Hernandez I, Sanz-Moreno V, Sumara I. UBASH3B-mediated silencing of the mitotic checkpoint: Therapeutic perspectives in cancer. *Mol Cell Oncol.* 2018;5:e1271494.
49. Artavanis-Tsakonas K, Weihofen WA, Antos JM, et al. Characterization and structural studies of the Plasmodium falciparum ubiquitin and Nedd8 hydrolase UCHL3. *J Biol Chem.* 2010;285:6857-6866.
50. Frickel EM, Quesada V, Muething L, et al. Apicomplexan UCHL3 retains dual specificity for ubiquitin and Nedd8 throughout evolution. *Cell Microbiol.* 2007;9:1601-1610.

SUPPORTING INFORMATION

Additional supporting information may be found online in the Supporting Information section.

How to cite this article: Jerabkova K, Liao Y, Kleiss C, et al. Deubiquitylase UCHL3 regulates bi-orientation and segregation of chromosomes during mitosis. *The FASEB Journal.* 2020;34:12751–12767. <https://doi.org/10.1096/fj.202000769R>